A&A 453, 121–132 (2006)
DOI: 10.1051/0004-6361:20054620

Astronomy & Astrophysics

Detection of K_s-excess stars in the 14 Myr open cluster NGC 4755

C. Bonatto[1], E. Bica[1], S. Ortolani[2], and B. Barbuy[3]

[1] Universidade Federal do Rio Grande do Sul, Instituto de Física, CP 15051, Porto Alegre 91501-970, RS, Brazil
e-mail: [charles;bica]@if.ufrgs.br
[2] Università di Padova, Dipartimento di Astronomia, Vicolo dell'Osservatorio 2, 35122 Padova, Italy
e-mail: ortolani@pd.astro.it
[3] Universidade de São Paulo, Rua do Matão 1226, 05508-900, São Paulo, Brazil
e-mail: barbuy@astro.iag.usp.br

Received 1 December 2005 / Accepted 20 February 2006

ABSTRACT

Aims. We derive the structure, distribution of MS and PMS stars and dynamical state of the young open cluster NGC 4755. We explore the possibility that, at the cluster age, some MS and PMS stars still present infrared excesses related to dust envelopes and proto-planetary discs.
Methods. J, H and K_s 2MASS photometry is used to build CMD and colour–colour diagrams, radial density profiles, luminosity and mass functions. Field-star decontamination is applied to uncover the cluster's intrinsic CMD morphology and detect candidate PMS stars. Proper motions from UCAC2 are used to determine cluster membership.
Results. The radial density profile follows King's law with a core radius $R_{\rm core} = 0.7 \pm 0.1$ pc and a limiting radius $R_{\rm lim} = 6.9 \pm 0.1$ pc. The cluster age derived from Padova isochrones is 14 ± 2 Myr. Field-star decontamination reveals a low-MS limit at $\approx 1.4\ M_{\odot}$. The core MF ($\chi = 0.94 \pm 0.16$) is flatter than the halo's ($\chi = 1.58 \pm 0.11$). NGC 4755 contains ∼285 candidate PMS stars of age ∼1−15 Myr, and a few evolved stars. The mass locked up in PMS, MS and evolved stars amounts to ∼1150 $M_{\odot}$. Proper motions show that K_s-excess MS and PMS stars are cluster members. K_s-excess fractions in PMS and MS stars are $5.4 \pm 2.1\%$ and $3.9 \pm 1.5\%$ respectively, consistent with the cluster age. The core is deficient in PMS stars, as compared with MS ones. NGC 4755 hosts binaries in the halo but they are scarce in the core.
Conclusions. Compared to open clusters in different dynamical states studied with similar methods, NGC 4755 fits relations involving structural and dynamical parameters in the expected locus for its age and mass. On the other hand, the flatter core MF probably originates from primordial processes related to parent molecular cloud fragmentation and mass segregation over ∼14 Myr. Star formation in NGC 4755 began ≈14 Myr ago and proceeded for about the same length of time. Detection of K_s-excess emission in member MS stars suggests that some circumstellar dust discs survived for $\sim 10^7$ yr, occurring both in some MS and PMS stars for the age and spread observed in NGC 4755.

Key words. Galaxy: open clusters and associations: individual: NGC 4755 – Galaxy: structure

1. Introduction

Before settling onto the zero-age main sequence (ZAMS), stars spend their early lives surrounded by optically thick material consisting of an infalling envelope and accretion disc that gradually disperse along the pre-main sequence (PMS) phase. The gas and dust disc and envelope (DDE) are reminiscent of the primordial gravitational collapse that formed the stars. Final stages of disc accretion may last as long as $\sim 10^7$ yr (White & Hillenbrand 2005) and the presence of such inner discs may be traced by observations in near-infrared bands.

On theoretical grounds it is estimated that because of disc-depleting processes such as irradiation by the central star, viscous accretion and mass loss due to outflow, the median lifetime of optically thick inner accretion discs may be as short as 2−3 Myr (Hillenbrand 2005). In fact, observations indicate that significant fractions of stars younger than 1 Myr have already lost their discs. However, they also indicate that 8–16 Myr old stars may still retain their inner discs (e.g. Chen et al. 2005; Low et al. 2005). Similar conclusions were reached by Armitage et al. (2003) who found that ∼30% of the stars in young clusters lose their discs in less than 1 Myr, while the remainder keep them for about 1–10 Myr. Observational estimates of disc survival time-scales are important for planet formation theories (Brandner et al. 2000).

Circumstellar discs in T Tauri stars have been inferred from infrared excesses originated in dust-heated emission (Hillenbrand 2005; Ortolani et al. 2005 and references therein). The current consensus is that near-infrared excesses correlate inversely with stellar age. Near-infrared colour–colour diagrams (2-CD) involving $JHKL$ or K_s-bands have been widely used to identify infrared-excess stars and candidate circumstellar discs in young clusters (Hillenbrand 2005; Lada & Adams 1992). Thus, detection of DDEs around stars in young clusters with accurate age determination is crucial to observationally constrain dust disc time-scales.

In addition to the disc-lifetime problem, stars in young open clusters do not all have the same age, but formed along some period of time (e.g. Sagar & Cannon 1995, and references therein). Inferences on star-formation time-scales may be made by comparing the age derived from the bulk of main sequence (MS) stars with that implied from the observed distribution of PMS stars. This in turn may provide constraints on the time-scale of the parent molecular cloud fragmentation.

Another issue associated with molecular cloud fragmentation is the apparent universality of the initial mass function (IMF). Observations of star-forming regions in molecular clouds, rich star clusters and Galactic field suggest that the IMF is similar in these very different environments (Kroupa 2002). This suggests that the initial distribution of stellar masses depends on the process of molecular cloud fragmentation. Fragmentation, in turn, should produce similar IMFs despite very different initial conditions, a not yet understood physical process (Kroupa 2002).

Detailed analysis of stellar density structure and stellar-mass distribution in young star clusters may shed light on these issues. Rich young clusters at the post embedded phase represent ideal targets because they contain large numbers of stars with different masses and provide uniformity in parameters such as age, chemical composition, distance and reddening. Assigning accurate ages to such clusters by means of theoretical isochrones is feasible because of evolved-star and/or PMS features in observed colour–magnitude diagrams (CMDs).

Recently, the structure and stellar distribution of the very young embedded open cluster NGC 6611 (age $\approx 1.3 \pm 0.3$ Myr) was analyzed with near-infrared CMDs and 2-CDs (Bonatto et al. 2006). Despite the young age, NGC 6611 presents signs of dynamical evolution, such as a mass function (MF) in the cluster core significantly flatter than the halo's. They suggested that such MF flattening in the core is probably associated with the parent molecular cloud fragmentation, where more massive proto-stars are preferentially located in the central parts, which agrees with Kroupa (2004) in the observed degree of mass segregation in clusters younger than a few Myr. In addition, NGC 6611 was shown to contain a significant number of PMS stars with ages in the range 0.2–4 Myr. Some of these PMS stars present infrared excess emission.

The rich open cluster NGC 4755, with an age in the range 10–20 Myr (e.g. Sanner et al. 2001; Nilakshi et al. 2002) and evidence of hosting PMS stars (e.g. Sagar & Cannon 1995), is another candidate to search for PMS stars and infrared excess emission. We will follow similar procedures as for the comparison open cluster NGC 6611.

Our goals with the present work are *(i)* to carry out a detailed analysis of the density structure of NGC 4755, *(ii)* analyze the core, halo and overall cluster MFs, *(iii)* derive properties of MS and PMS stars and cluster parameters, *(iv)* infer information on the dynamical state, and *(v)* search for infrared-excess stars at such ages. For spatial and photometric uniformity, we employ J, H and K_s 2MASS[1] photometry. The 2MASS Point Source Catalogue (PSC) is uniform reaching relatively faint magnitudes covering nearly all the sky, allowing a proper background definition for clusters with large angular sizes (e.g. Bonatto et al. 2005, 2004a).

This paper is organized as follows. In Sect. 2 we review previous results on NGC 4755. In Sect. 3 we present the 2MASS data, subtract field-star contamination, derive fundamental cluster parameters, discuss candidate PMS stars and analyze the cluster density structure. In Sect. 4 we derive luminosity functions (LFs) and MFs and discuss stellar content properties. In Sect. 5 we compare NGC 4755 with open clusters in different dynamical states. Concluding remarks are given in Sect. 6.

[1] The Two Micron All Sky Survey, All Sky data release (Skrutskie et al. 1997), available at
http://www.ipac.caltech.edu/2mass/releases/allsky/

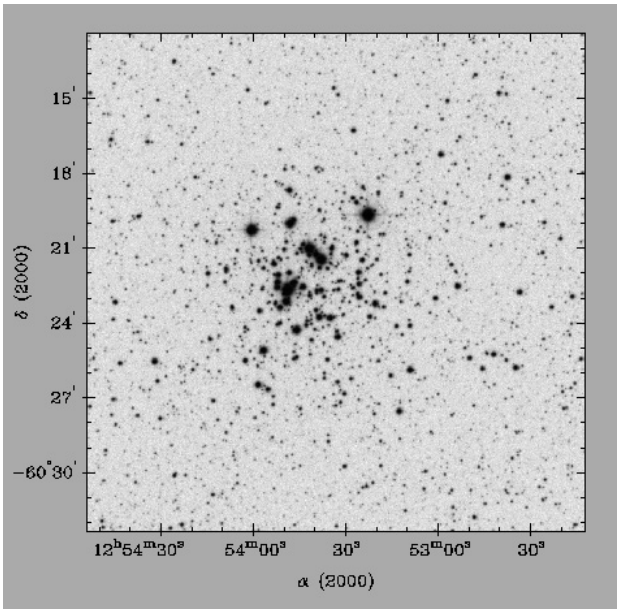

Fig. 1. DSS B image of NGC 4755 covering $20' \times 20'$.

2. The post-embedded open cluster NGC 4755

NGC 4755, also known as κ Crucis or *Herschell's Jewel Box*, is a prominent young open cluster in the southern hemisphere. The bright stars characterizing this cluster can be seen in the DSS[2] B image (Fig. 1) covering $20' \times 20'$. This cluster contains the red supergiant (SG) CPD − 59°4547 of spectral type M2Iab and $V = 7.45$ and $(B - V) = 2.22$ (Dachs & Kaiser 1984). They also classified 5 blue SGs with $5.7 < V < 9.1$ in NGC 4755. They detected several extremely red stars in the cluster field by means of UBV photometry. They have near-infrared counterparts in the present study, seen especially in a 2-CD (Sect. 3.4).

No evidence of gas emission or dust filaments appears in this B DSS image (such features are almost totally absent in the R XDSS image) of NGC 4755, which we refer to as a post-embedded young open cluster.

Lyngå (1987) classified NGC 4755 as Trumpler type I3r, with angular diameter $D = 10'$, and estimated a MS turn-off age in the range 7−24 Myr.

Sagar & Cannon (1995) using deep $UBVRI$ CCD photometry estimated a distance from the Sun $d_\odot \approx 2.1 \pm 0.2$ kpc. They found variable reddening following a normal extinction law with an average value $E(B - V) = 0.41$ and a differential reddening range $\Delta E(B - V) = 0.05$, a picture typical of a post-embedded young open cluster, where molecular and dust clouds are dissipating. This is consistent with the near absence of dust filaments in NGC 4755 (Fig. 1). They suggested that star-formation in the parent molecular cloud might have proceeded for at least 6−7 Myr, and massive stars ($m > 10\ M_\odot$) formed ~4 Myr before the bulk of the low-mass stars ($m < 2\ M_\odot$). They also detected PMS stars with ages in the range 3−10 Myr.

Based on BVI CCD photometry and astrometric data, Sanner et al. (2001) derived $d_\odot \approx 2.1 \pm 0.2$ kpc, $E(B - V) = 0.36 \pm 0.02$, an age of 10 ± 5 Myr, and an IMF with slope $\chi = 1.68 \pm 0.14$ for stars in the mass range $1.2 \leq m(M_\odot) \leq 13.6$. They derived a solar metallicity.

Using UBV CCD observations Tadross et al. (2002) derived for NGC 4755 a colour excess $E(B - V) = 0.38$, $d_\odot \approx 1.8$ kpc,

[2] Extracted from the Canadian Astronomy Data Centre (CADC), at
http://cadcwww.dao.nrc.ca/

age ≈ 34 Myr, linear diameter D = 5.4 pc, Galactocentric distance d_{GC} = 7.66 kpc, number of member stars N_* = 364, and cluster mass of m = 682 $M_\odot$.

Nilakshi et al. (2002) using photometry from Palomar Observatory Sky Survey I plates found $d_\odot \approx 2.1$ kpc, d_{GC} = 7.6 kpc, age ≈ 20 Myr, core radius $R_{core} = 0.63 \pm 0.10$ pc and core stellar density $\rho_c = 21.1 \pm 3.8$ stars pc^{-2}, halo radius R_h = 6.1 pc and halo stellar density $\rho_h = 7.4 \pm 0.3$ stars pc^{-2}.

Piskunov et al. (2004) using BV CCD photometry derived an age of 16 ± 1 Myr, IMF slope $\chi = 1.4 \pm 0.3$ and a star-formation spread of 1 ± 1 Myr.

In the WEBDA[3] open cluster database (Mermilliod 1996) the central coordinates of NGC 4755 are (J2000) $\alpha = 12^h53^m39^s$, and $\delta = -60°21'42''$. However, the radial density profile (Sect. 3.3) for these coordinates presented a dip at $R = 0'$. We searched for a new center by examining histograms for the number of stars in 0.5′ bins of right ascension and declination. The coordinates that maximize the density of stars at the center are (J2000) $\alpha = 12^h53^m33.1^s$, and $\delta = -60°22'21.0''$, corresponding to $\ell = 303.193°$ and $b = +2.498°$. In what follows we refer to these optimized coordinates as the center of NGC 4755. WEBDA gives $E(B-V) = 0.386$, $d_\odot$ = 1.98 kpc and age = 16 Myr.

3. Cluster parameters from 2MASS data

VizieR[4] was used to extract J, H and K_s 2MASS photometry in a circular area with radius $R = 50'$ centered on the optimized coordinates of NGC 4755 (Sect. 2). As a photometric quality constraint, the extraction was restricted to stars brighter than the 99.9% Point Source Catalogue Completeness Limit[5], J = 15.8, H = 15.1 and K_s = 14.3, respectively. For reddening transformations we use the relations $A_J/A_V = 0.276$, $A_H/A_V = 0.176$ and $A_{K_s}/A_V = 0.118$ (Dutra et al. 2002), assuming a total-to-selective absorption ratio $R_V = 3.1$.

The CMD of the central 10′ of NGC 4755 is given in Fig. 2. Reflecting the young age, a prominent, nearly vertical MS is present, together with a single bright star at $J \approx 3$ and $(J-H) \approx 0.95$ (the red SG CPD − 59°4547). Because of its low latitude, field stars (mostly disc) contaminate the CMD, particularly at faint magnitudes and red colours mimicking a MS extending to sub-solar mass stars, which is not compatible with a 10–20 Myr old cluster.

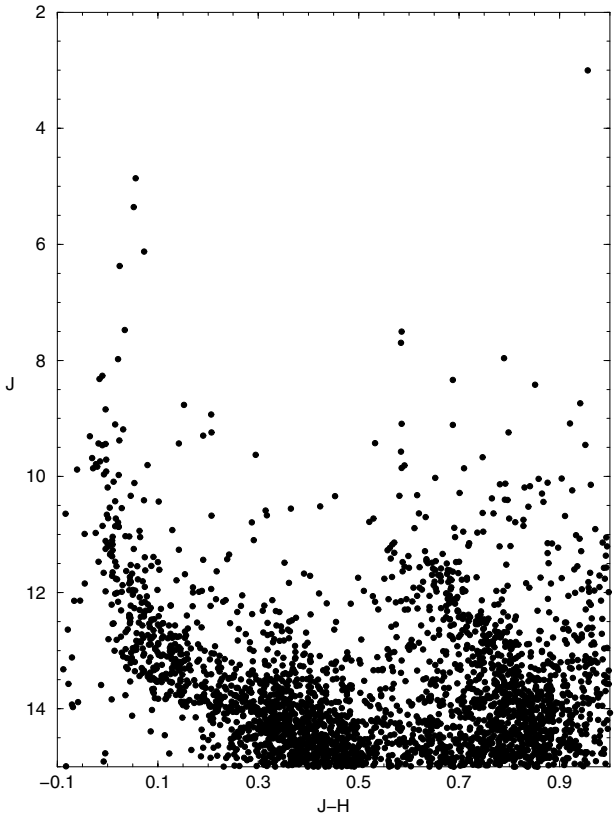

Fig. 2. $J \times (J-H)$ CMD of the central 10′ of NGC 4755 (blue sequence). Field-star contamination, mostly by disc stars, is conspicuous. The extension of the MS to $J < 14$ appears to be a field-star contamination artifact.

3.1. Field-star decontamination

The relative density and colour–magnitude distribution of the field-star contamination can be evaluated in the left panel of Fig. 3 where we superimpose on the observed CMD of the central 10′ the corresponding (same area) field-star contribution. Most of the faint ($J \leq 14$) and red ($(J-H) \geq 0.5$) stars probably are contaminant field stars. To retrieve the intrinsic cluster-CMD morphology we use a field-star decontamination procedure previously applied in the analysis of low-contrast (Bica & Bonatto 2005b) and young embedded (Bonatto et al. 2006) open clusters. As the offset field we take the region located at $30' \leq R \leq 50'$. This area is large enough to produce field-star statistical representativity (≈78 000 stars), both in magnitude and colours.

Based on the spatial number-density of stars in the offset field, the decontamination procedure estimates the number of field stars that within the 1σ level are expected to be present in the cluster field. The observed CMD is divided in colour/magnitude cells from which stars are randomly subtracted in a number consistent with the expected number of field stars in the same cell. Dimensions of the colour/magnitude cells can be subsequently changed so that the total number of stars subtracted throughout the whole cluster area matches the expected one, at the 1σ level. Since field stars are taken from an external region of fixed dimension, corrections are made for differences in solid angle between cluster and offset field regions. This procedure can be applied to the whole cluster and internal regions as well. Because it actually excludes stars from the original files – thus artificially changing both the radial distribution of stars and LFs – we use field-star decontamination only to uncover the intrinsic CMD morphology and build 2-CDs.

The number of observed stars in the central 10′ field of NGC 4755 is 5510. Since the field-star ($30' \leq R \leq 50'$) density is 13.6 ± 0.15 stars $(')^{-2}$ the expected number of cluster stars in that region amounts to 1246 ± 99 (22.6%), while field stars are 4264 ± 65 (77.4%). These numbers were obtained with colour/magnitude cells of dimensions 0.01 and 0.025, respectively.

The field-star decontaminated CMD of the central 10′ is in the right panel of Fig. 3. As expected, most of the faint and red stars were eliminated by the decontamination procedure. The decontaminated CMD morphology presents an extended,

[3] http://obswww.unige.ch/webda

[4] http://vizier.u-strasbg.fr/viz-bin/VizieR?-source=II/246

[5] Following the Level 1 Requirement, according to http://www.ipac.caltech.edu/2mass/releases/allsky/doc/sec6_5a1.html

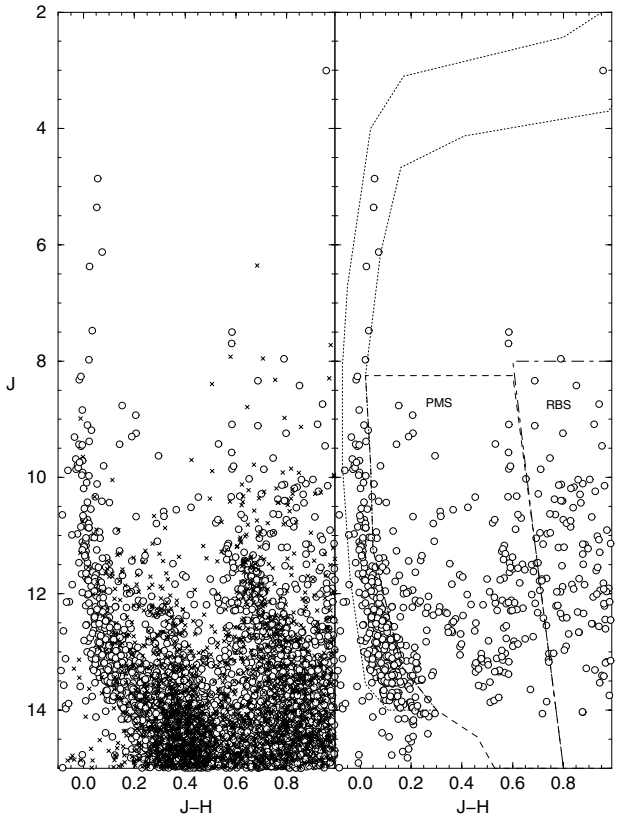

Fig. 3. *Left panel*: field stars ("×") are superimposed on the observed CMD of the central 10′ of NGC 4755. Extraction areas match. *Right panel*: field-star decontaminated CMD. Colour filters used to isolate MS (dotted lines), candidate-PMS (dashed) and very red (dot-dashed) stars are shown.

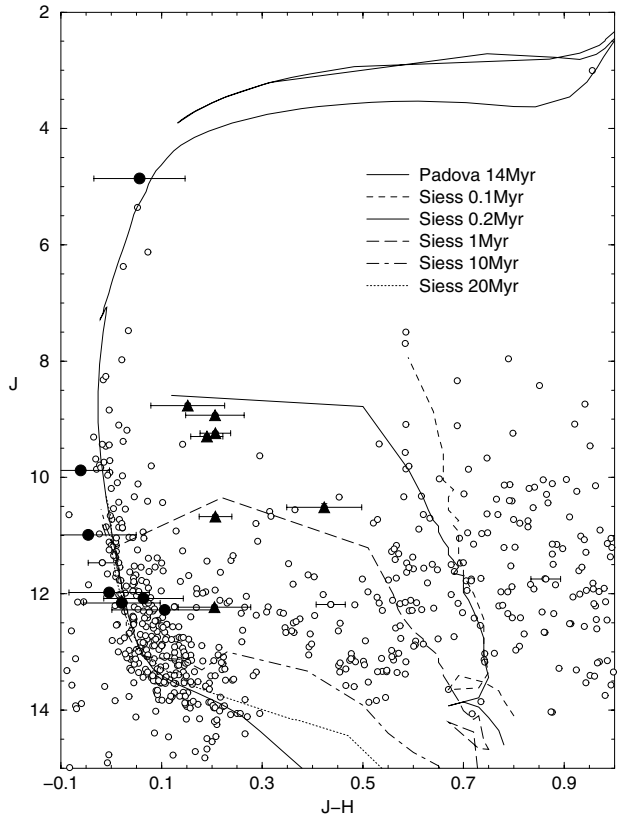

Fig. 4. Isochrone fit of the decontaminated CMD of the central 10′ of NGC 4755. The best fit was obtained with the 14 Myr solar-metallicity Padova isochrone, $E(J-H) = 0.07$ and $(m-M)_J = 11.5$. PMS tracks (0.1, 0.2, 1, 10 and 20 Myr) are plotted following the same $(m-M)_J$ and $E(J-H)$ solution. K_s-excess MS (filled circles) and PMS (filled triangles) stars are shown along with the individual error bars (Sect. 3.4.1). To avoid cluttering, only representative error bars are shown for non-K_s-excess stars.

nearly-vertical MS with the faint-limit at $J \approx 14$. It suggests the presence of a significant population of candidate PMS stars at $0.2 \leq (J-H) \leq 0.8$, and a number of very red stars at $(J-H) \geq 0.8$ that are probably red background stars (RBS – Sect. 3.4). Indeed, the presence of background disc stars is expected in the direction of NGC 4755, since we are observing at $\ell \approx 303°$ and low latitude. In Fig. 3 we show the colour–magnitude filters used to isolate MS/evolved, candidate PMS and RBS stars. The filters were defined based on the distribution of the decontaminated star sequences as compared with theoretical MS and PMS tracks (Fig. 4). The MS filter follows the 14 Myr Padova isochrone (Sect. 3.2) allowing for photometric uncertainties, while the PMS filter describes the colour/magnitude space covered by the 0.1–20 Myr PMS tracks (Sect. 3.4). The MS/evolved, candidate-PMS and RBS colour-filters applied to the observed photometry of the central 10′ field (left panel of Fig. 3) select 346, 1131 and 953 stars, respectively. Applied to the field-star decontaminated photometry (right panel of Fig. 3), the filters select 277 (80 ± 6% of the observed ones), 285 (25 ± 2%) and 204 (21 ± 2%) stars, respectively for MS/evolved, candidate-PMS and RBS stars.

3.2. Cluster age and distance from the Sun

Cluster age is derived with solar-metallicity Padova isochrones (Girardi et al. 2002) computed with the 2MASS J, H and K_s filters[6].

It is usually difficult to derive age by means of CMDs for young star clusters because of nearly-vertical MS and scarcity of evolved stars. The lack of observational CMD constraints allows several age solutions. In the field-star decontaminated CMD of NGC 4755 the red SG together with the rather well-defined low-MS reaching $J \approx 14$ constrain the age to 14 ± 2 Myr. Parameters derived from the isochrone fit are the observed distance modulus $(m-M)_J = 11.5 \pm 0.1$ and colour excess $E(J-H) = 0.07 \pm 0.01$, converting to $E(B-V) = 0.22 \pm 0.03$. This age solution is plotted in Fig. 4. With these parameters the absolute distance modulus is $(m-M)_O = 11.3 \pm 0.1$, resulting in $d_\odot = 1.8 \pm 0.1$ kpc. The Galactocentric distance of NGC 4755 is $d_{GC} = 7.2 \pm 0.2$ kpc, using 8.0 kpc as the Sun's distance to the Galactic center (Reid 1993). MS stars are restricted to the mass range $1.4 \leq m(M_\odot) \leq 13.5$.

3.3. Cluster structure

Cluster structure was inferred by means of the radial density profile (RDP), defined as the projected number-density of cluster stars around the center. The MS/evolved RDP was built with stars selected after applying the respective colour-magnitude filter shown in Fig. 3. Within uncertainties, the filter describes the cluster's intrinsic CMD morphology from the upper MS/evolved

[6] `http://pleiadi.pd.astro.it/isoc_photsys.01/isoc_photsys.01.html`. 2MASS transmission filters produced isochrones very similar to the Johnson ones, with differences of at most 0.01 in $(J-H)$ (Bonatto et al. 2004b).

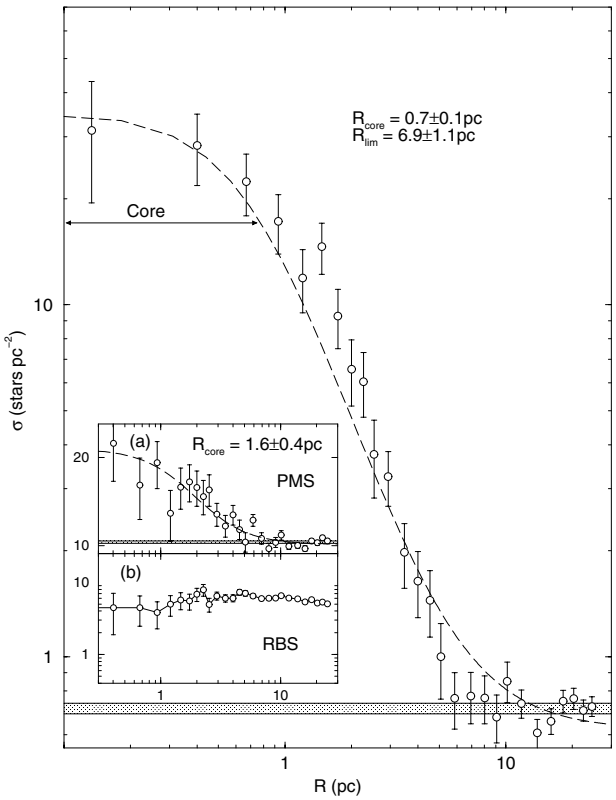

Fig. 5. Radial density profile (MS) of NGC 4755. Dashed line: two-parameter King profile; core size is indicated. Shaded region: stellar background level. Insets: RDP of PMS (panel **a**)) and RBS (panel **b**)) stars.

stars to the turn-on region at $J \approx 14$. This procedure allowed us to exclude most of the background field objects. The use of colour–magnitude filters to discard stars with discordant colours was previously applied in the analysis of the open clusters M 67 (Bonatto & Bica 2003), NGC 188 (Bonatto et al. 2005) and NGC 3680 (Bonatto et al. 2004a). To avoid oversampling near the center and undersampling for large radii, the RDP was built counting stars in rings with radius $\Delta R = 0.5'$ for $0 \leq R(') < 5$, $\Delta R = 1'$ for $5 \leq R(') < 10$, $\Delta R = 2'$ for $10 \leq R(') < 20$ and $\Delta R = 4'$ for $R \geq 20'$. The residual background level corresponds to the average number of stars in the region located at $28' \leq R \leq 46'$, resulting in $\sigma_{\rm bg} = 0.203 \pm 0.007$ stars $(')^{-2}$.

Figure 5 shows the MS/evolved stars' RDP. For absolute comparison between clusters the radius scale was converted to parsecs and the number-density of stars to stars pc^{-2} using the distance derived in Sect. 3.2. The high statistical significance of the RDP is reflected in the 1σ Poisson error bars.

Structural parameters of NGC 4755 were derived by fitting the two-parameter King (1966a) surface density profile to the background-subtracted RDP. King's model describes the intermediate and central regions of normal clusters (King 1966b; Trager et al. 1995). The fit was performed using a nonlinear least-squares fit routine that uses errors as weights. The best-fit solution (Fig. 5) is superimposed on the observed RDP. Parameters derived are King's background-subtracted central density of stars $\sigma_{0\rm K} = 9.9 \pm 1.4$ stars $(')^{-2} = 34.8 \pm 5.1$ stars pc^{-2}, and core radius $R_{\rm core} = 1.38 \pm 0.15' = 0.74 \pm 0.08$ pc. Considering fluctuations of the observed RDP with respect to the background the cluster extends up to a limiting radius $R_{\rm lim} = 13 \pm 2' = 6.9 \pm 1.1$ pc. $R_{\rm lim}$ describes where the observed RDP merges into the background and for practical purposes the bulk of the cluster stars are contained within $R_{\rm lim}$. The present values of $R_{\rm core}$ and $R_{\rm lim}$ agree at the 1σ level with those of Nilakshi et al. (2002).

To determine membership we also build RDPs for stars located in the PMS and RBS CMD regions (Fig. 3). Both sets of stars were isolated by the respective colour–magnitude filters. Despite large errors, the RDP of PMS stars is well fitted by a King's profile with $\sigma_{0\rm K} = 11.3 \pm 2.6$ stars pc^{-2} and core radius $R_{\rm core} = 1.6 \pm 0.4$ pc. This value of $R_{\rm core}$ differs $\sim 2\sigma$ from that derived with MS/evolved stars, while the central number-density of PMS stars is $\sim 1/3$ of that of the MS stars. Both the difference in core radius and number-density with respect to MS stars suggest a deficiency of PMS stars in the core (Sect. 4.2). The PMS limiting radius $R_{\rm lim} = 8 \pm 1$ pc agrees with the MS/evolved one. We conclude that cluster membership of the candidate-PMS stars is statistically indicated by their RDP (panel a) that presents a similar limiting radius as that of the MS/evolved stars and is represented well by King's profile.

On the other hand, the nearly flat RDP of RBS stars (panel b) represents that expected from the background.

King's profile provides a good fit to the stellar RDP of NGC 4755, particularly for MS/evolved stars. Since it follows from an isothermal (virialized) sphere, the close similarity of the stellar RDP with a King profile may suggest that the internal structure of NGC 4755 (particularly the core) has reached some level of energy equipartition after $\sim$14 Myr. Part of this effect may be linked to molecular cloud fragmentation (Sect. 5), similarly to NGC 6611 (Bonatto et al. 2006).

3.4. Candidate pre-main sequence stars

A significant number of stars to the right of the MS remains in the decontaminated CMD (Figs. 3 and 4). In young open clusters this CMD region is usually occupied by PMS stars. To characterize these stars in terms of age and mass we use PMS tracks of Siess et al. (2000) with ages 0.1, 0.2, 1, 10 and 20 Myr (the 0.1 Myr track is used to mark off the red PMS threshold). To these tracks we apply the $(m - M)_J$ and $E(B - V)$ values derived from the Padova isochrone fit (Sect. 3.2). The PMS tracks are given in Fig. 4. Candidate PMS stars are contained within the 1 Myr and 20 Myr tracks, and the turn-on points of the 10 and 20 Myr PMS tracks coincide with the MS low-mass limit ($\approx 1.4\ M_\odot$). Within uncertainties, cluster age – or at least the age of the earliest star formation event in NGC 4755 – implied by the oldest PMS turn-on points is consistent with that derived with the Padova isochrone. The coincidence in age of the oldest PMS turn-on with the MS, together with the PMS age spread, indicates that star formation in NGC 4755 began $\sim$14 Myr ago and proceeded for about the same time.

Properties of stars in the field of NGC 4755 are also inferred by means of the 2-CD $(H - K_s) \times (J - H)$, built with foreground reddening-corrected photometry of the central $10'$ region (Fig. 6). To minimize photometric uncertainties and/or spurious detections we restricted the analysis to stars brighter than $J = 13$, taken from the field-star decontaminated photometry (Sect. 3.1). At this magnitude range we are probing stars more massive than $\approx 2\ M_\odot$. Mean photometric errors for MS, PMS and RBS stars are shown. For comparison we plot the 14 Myr Padova isochrone restricted to the magnitude range $J = 13$ to the turnoff (≈ 2.0–$13.5\ M_\odot$), the 10 Myr PMS track and the MS and giants loci of Schmidt-Kaler (1982). Schmidt-Kaler's MS includes stars more massive than $\approx 0.2\ M_\odot$. Except for low-mass stars the 10 Myr PMS track and Schmidt-Kaler's MS are coincident. To characterize colour excesses we use the OV/late dwarfs

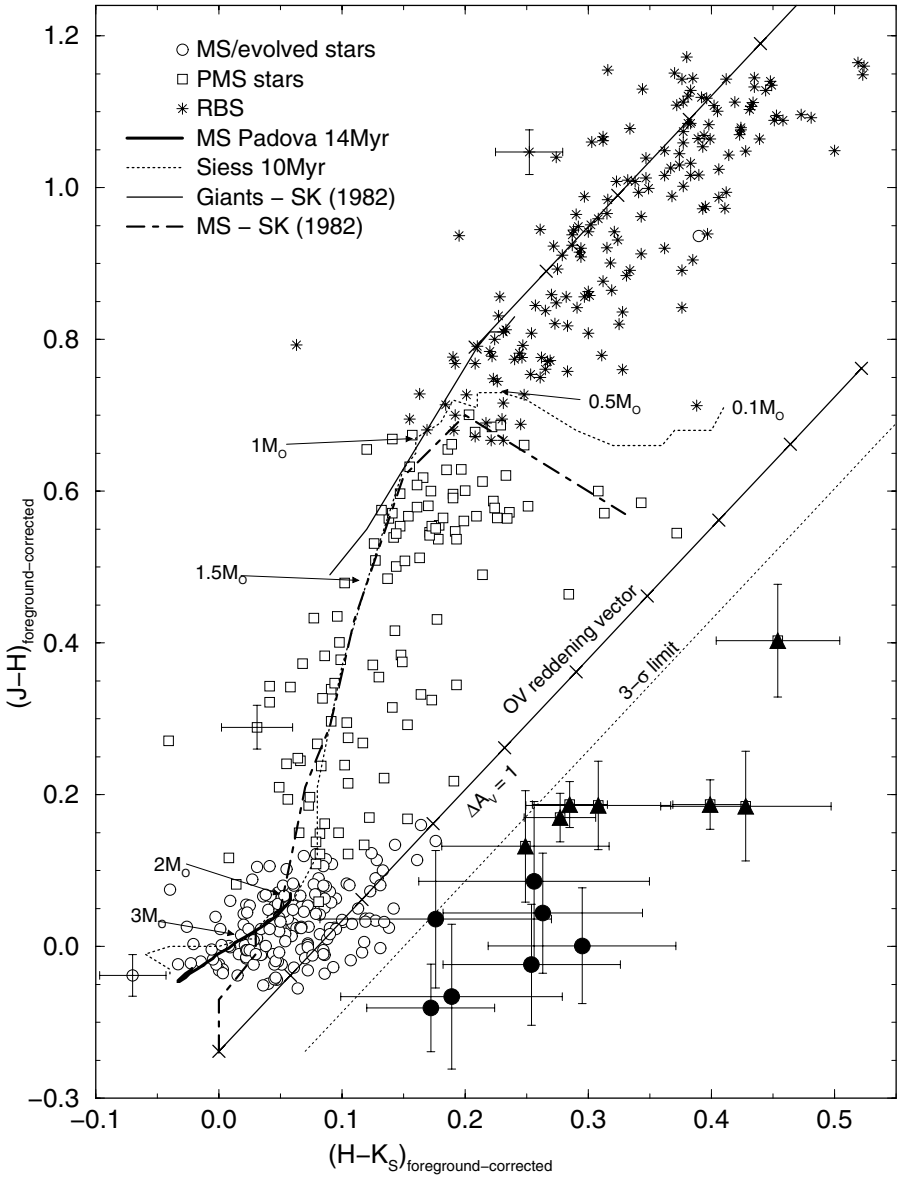

Fig. 6. Foreground reddening-corrected ($E(J-H) = 0.07$ and $E(H-K_s) = 0.04$)) 2-CD of the field-star decontaminated 10′ central region of NGC 4755. Photometry was restricted to $J \leq 13$. Circles: MS/evolved stars. Squares: PMS stars. Black stars: RBS. Heavy-solid line: 14 Myr Padova MS, restricted to $2.0 \leq m(M_\odot) \leq 13.5$. Dotted line: 10 Myr PMS track; representative PMS stellar masses are indicated. MS (dot-dashed line) and giant (solid) tracks are from Schmidt-Kaler (1982). Extinction vectors are shown with $\Delta A_V = 1$ mag subdivisions. Mean error bars in colour are shown for MS, PMS and RBS stars. K_s-excess MS (filled circles) and PMS (filled triangles) stars are to the right of the 3σ-limit line (light-dotted).

reddening vector that is based on Schmidt-Kaler's loci. Reddening vectors follow the relation $E(J-H) = 1.72 \times E(H-K_s)$ (Sect. 3). As expected, reddening-corrected MS stars distribute about the Padova isochrone (and Schmidt-Kaler's MS for $m > 2\ M_\odot$), but with a redward bias probably resulting from uncorrected photospheric reddening and some amount of K_s-excess emission. Most of the candidate PMS stars follow the 10 Myr track at the $\approx 1\sigma$ level and are bluer than the OV reddening vector. A few MS and candidate-PMS stars present K_s-excess.

Differential reddening cannot account for the large dispersion in colour observed in the CMD and 2-CDs (Figs. 4 and 6, respectively), since throughout the field of NGC 4755 it amounts to $\Delta E(B-V) = 0.05$ (Sagar & Cannon 1995).

As a further check on the reddened disc nature of the RBS stars we fitted a straight line to their colour–colour distribution. The resulting slope matches that of the reddening vector at the 1σ level.

The presence of member-PMS stars of different ages indicates that star formation in NGC 4755 did not occur as a single event about 14 Myr ago. Instead, massive stars and most of those more massive than $\sim 2\ M_\odot$ probably formed in the early collapse, but the time-scale for the formation of low-mass stars seems to be $\sim 10^7$ yr.

3.4.1. K_s-excess emission stars

Disc strength as measured by excesses in intrinsic $(H-K)$ or $(K-L)$ (or K_s) colours depends on stellar mass and radius, and disc properties such as accretion rate and geometry (D'Alessio et al. 1999). In particular, $(H-K_s)$ is sensitive to

discs with high accretion rates and low inclinations (Hillenbrand 2005).

In the present case we quantify disc strength by the fraction of stars with intrinsic K_s-excess (f_{K_s}). Intrinsic colour excesses are obtained by subtracting the foreground reddening from the observed colours, and applying a correction for the underlying stellar photosphere. Since we do not have photospheric corrections for each MS and PMS star we take as intrinsic K_s-excess stars those with the foreground-reddening corrected colour $(H - K_s)$ redder than the OV reddening vector by $\Delta(H-K_s) \approx 3\sigma \approx 0.06$ mag. According to this condition defined by the envelope of the reddest PMS stars (Fig. 6), 14 K_s-excess stars are detected in this 14 Myr old cluster. Half of them belong to the MS and the remainder to the PMS. We emphasize that these K_s-excess stars were taken from a field-star decontaminated sample of 2MASS stars brighter than $J = 13$. This restriction also precludes spurious measurements. Individual errors for these stars are shown in Fig. 6. Although with errors larger than the mean, the loci occupied by the K_s-excess stars are consistent with the selection criterion adopted above.

The K_s-excess stars above do not occupy the classical disc locus of unreddened T Tauri stars; instead they are somewhat bluer, particularly in $(J - H)$. However, theoretical models of classical full discs (e.g. Lada & Adams 1992) predict colour excesses that cover this region. These models extend to higher photospheric temperatures (to include Ae/Be stars), which in turn produce bluer colours. Alternatively, part of the excess blue colour might be related to disc evolution, since as discs age the inner regions are believed to dissipate more rapidly than the outer parts, creating central clearings. The role of central clearings in producing colours bluer than those of T Tauri stars should be investigated by modelling disc evolution. To further investigate the blue $(J - H)$ colours of the K_s-excess stars in NGC 4755 we compared 2MASS and Kenyon & Hartmann's (1995) IR photometry of stars in the Taurus-Auriga region. We found that the number of stars with blue colours in 2MASS is not larger than in Kenyon & Hartmann's (1995) photometry, which indicates that the probability of blue colours in 2MASS is similar to other standard photometries. Also, Taurus-Auriga stars with colours below those of classical T Tauri stars present millimeter-emission from wide discs (Andrews & Williams 2005).

Despite the present photometric quality constraints we cannot completely rule out observational errors and/or anomalous colours. Variability, however, is not a problem, since the J, H and K_s photometry was obtained on the same night, as quoted in 2MASS.

One possible conclusion is that most of the K_s-excess stars in NGC 4755 have a peculiar, hot full disc, and that at least the 4 bright stars (at $(J - H) \approx 0.19$ and $J \approx 9$ – Fig. 4) could be Ae/Be stars, being also quite luminous. Most of the considerations on the relation of circumstellar discs with colour have been based on observations of star clusters significantly younger than the 14 Myr old NGC 4755.

Bearing in mind the above caveats we estimate K_s-excess fractions of $f_{K_s} = 3.9 \pm 1.5\%$ and $f_{K_s} = 5.4 \pm 2.1\%$ for MS and PMS stars. Uncertainties were estimated assuming statistical Poisson distributions for the field-star decontaminated MS and PMS populations. Such low values of f_{K_s} are consistent with the age of NGC 4755, according to the age $\times$ f_{K_s} diagram (Hillenbrand 2005). A less conservative criterion for selecting K_s-excess stars, extending bluewards to the OV reddening vector, could double the f_{K_s} of MS stars, but would not change the value for PMS stars. The fractions would still be consistent with the cluster age.

MS and PMS K_s-excess emission stars detected in the 2-CD (Fig. 6) are identified in the field-star decontaminated CMD (Fig. 4). The K_s-excess MS stars are distributed about the expected MS locus, including 1 massive star.

We conclude that the field-star decontaminated CMD and 2-CD present some MS and PMS stars with K_s-excess emission. If the bulk of present-day MS stars in NGC 4755 formed shrouded by dust ∼14 Myr ago, at least ∼5% of the primordial circumstellar optically thick discs survives to date. This timescale for dust-disc survival seems to agree with the disc fractions based on 24 μm Spitzer Space Telescope data of Chen et al. (2005) and Low et al. (2005), and the disc-lifetime estimate of Armitage et al. (2003). As a caveat we note that since discs may dissipate from the inside out, the detection rate of dust discs at longer wavelengths is not necessarily the same as that implied by shorter wavelength observations, which are sensitive to hotter dust.

3.5. UCAC2 proper motions

Cluster membership of MS, candidate-PMS and RBS stars (Figs. 4 and 6) can be further checked by means of proper motion (PM) data.

Proper motion components in right ascension ($\mu_\alpha \times \cos(\delta)$) and declination ($\mu_\delta$) for stars in the field of NGC 4755 were obtained in UCAC2[7]. Rather than examining separately PM components we use the modulus of the projected PM on the sky $\mu(\mathrm{mas\ yr^{-1}}) = \sqrt{(\mu_\alpha \times \cos(\delta))^2 + \mu_\delta^2}$ (Bica & Bonatto 2005a). To be consistent with the 2MASS analysis PM data were extracted inside an area of 50′ in radius centered on the optimized coordinates of NGC 4755 (Sect. 2). Since UCAC2 also includes 2MASS photometry we verified that the correspondence between both catalogues is nearly complete for $7 \leq J \leq 14$. The few bright stars of NGC 4755 are not included in UCAC2.

To isolate the intrinsic PM distribution we take into account the background contamination by first applying the MS/evolved, PMS and RBS colour–magnitude filters (Fig. 3) to the regions $r \leq 10'$ (cluster) and $30' \leq r \leq 50'$ (offset field). The region $r \leq 10'$ or ≈5.3 pc, that matches the limiting radius of NGC 4755 (Sect. 3.3), provides an optimized density contrast between cluster and offset field (Fig. 5). Next we build histograms with the number of MS/evolved, PMS and RBS stars in PM bins of 2 mas yr^{-1} width, both for cluster and offset regions. Offset field histograms are scaled to match the projected cluster area. Finally, the residual field-star contamination is statistically eliminated by subtraction of the offset field histogram from that of the cluster for MS/evolved, PMS and RBS stars. The intrinsic PM distribution functions ($\phi(\mu) = \frac{\mathrm{d}N}{\mathrm{d}\mu}$) are given in Fig. 7.

The PM distribution of MS stars (panel a) presents a peak at $\mu \approx 5$ mas yr^{-1} and a secondary one at $\mu \approx 11$ mas yr^{-1}. As discussed in Bica & Bonatto (2005a), the low-velocity peak is a consequence of the random collective motion of single stars superimposed on the cluster's systemic motion. The high-velocity peak is associated with unresolved binary (and multiple) systems, where the presence of a secondary changes appreciably the velocity of the primary star. This effect was shown for M 67 in Bica & Bonatto (2005a). The binary peak is also present in NGC 3680 (Bonatto et al. 2004a).

[7] The Second US Naval Observatory CCD Astrograph Catalog (Zacharias et al. 2003), available at
http://vizier.u-strasbg.fr/viz-bin/VizieR?-source=UCAC2

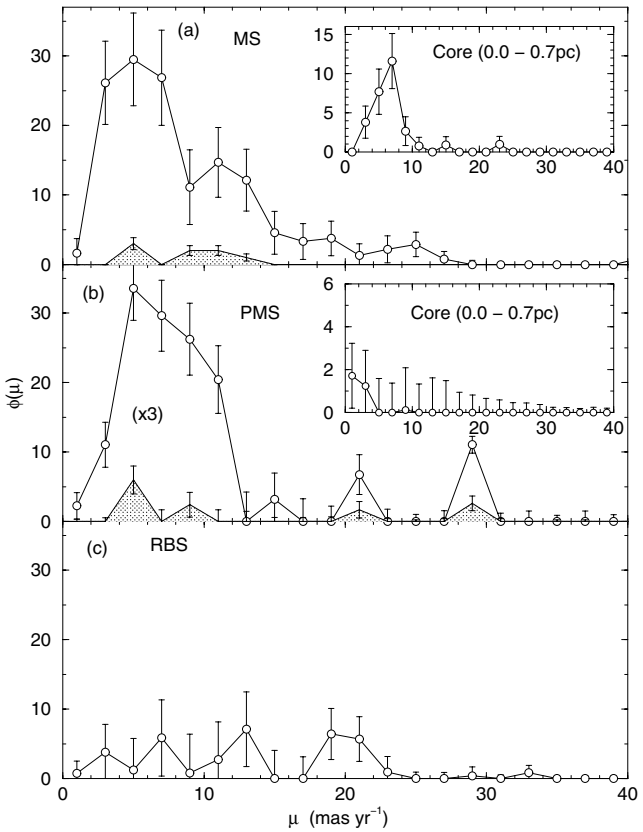

Fig. 7. Intrinsic proper motion distribution functions of MS (panel **a)**), PMS (panel **b)**) and RBS (panel **c)**) stars. Shaded curves: distribution of K_s-excess MS (panel **a)**) and PMS (panel **b)**) stars. The spatial region in panels **a)**–**c)** is $R \leq 10'$ ($R \leq 5.3$ pc). Insets: respective PM distributions in the MS core ($R \leq 0.74$ pc). No K_s-excess star was found in the core. The scale in panel **b)** was multiplied by 3.

Considering error bars, the PM distribution of PMS stars (panel b) shows an excess over the field stars for $\mu \leq 13$ mas yr^{-1} that coincides with the range in PM covered by the single and binary-star peaks of the MS distribution (panel a). This reinforces cluster membership of the candidate-PMS stars.

The PM distribution of RBS stars, on the other hand, represents Poisson fluctuations of field stars, which agrees with the RDP analysis (Sect. 3.3).

In Fig. 7 we also analyze PM distributions of K_s-excess MS and PMS stars. Considering the small number of these objects, we conclude that K_s-excess MS stars share essentially the same PM distribution as the combined (with and without K_s-excess) MS single stars. A similar conclusion applies to the K_s-excess PMS stars. Together with their locus in the field-star decontaminated CMD (Fig. 4), PM analysis confirms cluster membership of the K_s-excess MS and PMS stars.

The PM distribution of MS stars in the core ($R \leq 0.74$ pc) of NGC 4755 (inset of panel a) presents a low-velocity (single-star) peak. This suggests that the fraction of binaries in the core is not significant, as compared with that in the halo. The inset of panel (b) shows that the PM distribution of the PMS stars in the core of NGC 4755 presents evidence of a low-velocity peak. To avoid inconsistency in spatial regions we only consider the PMS stars found in the MS core ($R \leq 0.74$ pc). The large uncertainties preclude further analysis. The core contains no K_s-excess MS or PMS stars.

4. Luminosity and mass functions

To analyze the spatial dependence of LFs and MFs $\left(\phi(m) = \frac{dN}{dm}\right)$ in NGC 4755 we consider the regions: *(i)* – core ($0.0 \leq R$(pc) ≤ 0.74), *(ii)* halo ($0.74 \leq R$(pc) ≤ 6.94), and *(iii)* overall cluster ($0.0 \leq R$(pc) ≤ 6.94). To maximize the statistical significance of field-star counts we take as the offset field the region at $15 \leq R$(pc) ≤ 25, that lies ≥8 pc beyond the limiting radius.

First we isolate MS stars with the colour–magnitude filter (Fig. 3) in the range $7 \leq J \leq 14$. The filtering takes into account most of the field stars, leaving a residual contamination. We deal with this statistically by building LFs for each cluster region and offset field separately. The faint-magnitude limit of the MS is significantly brighter than that of the 99.9% Completeness Limit (Sect. 3). J, H and K_s LFs are built by counting stars in magnitude bins from the respective faint magnitude limit to the turn-off, for cluster and offset field regions. To avoid undersampling near the turn-off and oversampling at the faint limit, magnitude bins are wider in the upper MS than in the lower MS. Corrections are made for different solid angles between offset field and cluster regions. Intrinsic LFs are obtained by subtracting the respective offset-field LFs (Fig. 8). Finally, the intrinsic LFs are transformed into MFs using the mass-luminosity relation obtained from the 14 Myr Padova isochrone and observed distance modulus $(m - M)_J = 11.5$ (Sect. 3). These procedures are applied independently to the three 2MASS bands. The final MFs are produced by combining the J, H and K_s MFs. Figure 8 shows core, halo and overall MFs, covering the mass range $1.4 \leq m(M_\odot) \leq 13.5$. To these MFs we fit the function $\phi(m) \propto m^{-(1+\chi)}$. The fits are shown in Fig. 8, and MF slopes in Table 1. PMS stars are scarce in the core compared to the halo.

Both the overall and halo MFs are slightly steeper than Salpeter's (1955) IMF ($\chi = 1.35$) with slopes $\chi = 1.43 \pm 0.08$ and $\chi = 1.58 \pm 0.11$. However, the core MF is flatter, with $\chi = 0.94 \pm 0.16$. The increase in MF slope from core to halo may reflect some amount of mass segregation in the core. We discuss this point further in Sect. 5.

4.1. Observed cluster mass

Table 1 presents parameters derived from the core, halo and overall MFs. The number of evolved stars (Col. 2) in each region of NGC 4755 was obtained by integration of the respective field-star subtracted LF ($J \leq 7$). Multiplying this number by the mass at the turn-off ($m \approx 13.5\ M_\odot$) yields an estimate of the mass stored in evolved stars (Col. 3). PMS stars were isolated by means of the PMS colour-filter (Fig. 3). The number of PMS stars (Col. 4) was estimated similarly as for the evolved stars. Based on the observed distribution of PMS stars, evolutionary tracks (Fig. 4) and the fact that MFs in general increase in number for the subsolar-mass range, we assume an average PMS mass of 1 $M_\odot$. The mass stored in PMS stars is given in Col. 5. The observed number of MS stars and their corresponding mass (Cols. 7 and 8, respectively) were derived by integrating the MF in the mass range 1.4–13.5 $M_\odot$. To these we add the corresponding values of number and mass of PMS and evolved stars to derive the total number of observed stars (Col. 9), observed mass (Col. 10), projected mass density (Col. 11) and mass density (Col. 12). The mass locked up in MS/evolved and PMS stars in NGC 4755 is ∼1150 $M_\odot$, ∼16% of this stored in the core. For the PMS stars we estimate a mass of ≈285 $M_\odot$.

The present mass determination for NGC 4755 is a factor ≈1.7 of that of Tadross et al. (2002) and ≈0.7 the mass in NGC 6611 (Bonatto et al. 2006). The above mass and density

Table 1. Parameters derived from MFs and PMS stars of NGC 4755.

	Evolved		PMS		Observed MS			Observed MS + PMS + Evolved				τ
Region	N^*	m	N^*	m	$\chi_{1.4-13}$	N^*	m_{obs}	N^*	m	σ	ρ	
	(stars)	($M_\odot$)	(stars)	($M_\odot$)		(10^2 stars)	(10^2 $M_\odot$)	(10^2 stars)	(10^2 $M_\odot$)	($M_\odot$ pc^{-2})	($M_\odot$ pc^{-3})	
(1)	(2)	(3)	(4)	(5)	(6)	(7)	(8)	(9)	(10)	(11)	(12)	(13)
Core	1 ± 1	14 ± 14	9 ± 2	9 ± 2	0.94 ± 0.16	0.4 ± 0.1	1.2 ± 0.4	0.5 ± 0.1	1.5 ± 0.4	85 ± 22	86 ± 23	40 ± 9
Halo	4 ± 2	54 ± 27	278 ± 83	278 ± 83	1.58 ± 0.11	2.2 ± 0.3	6.4 ± 1.1	5.0 ± 0.9	9.7 ± 1.4	6.5 ± 0.9	0.7 ± 0.1	–
Overall	5 ± 2	68 ± 27	285 ± 85	285 ± 85	1.43 ± 0.08	2.6 ± 0.3	8.0 ± 1.1	5.5 ± 0.9	11.5 ± 1.4	7.6 ± 0.9	0.8 ± 0.1	0.6 ± 0.1

Notes. Observed mass range: 1.5−13.4 $M_\odot$. Column 6 gives the MF slope derived for MS stars. Column 13: dynamical-evolution parameter τ = age/t_{relax}.

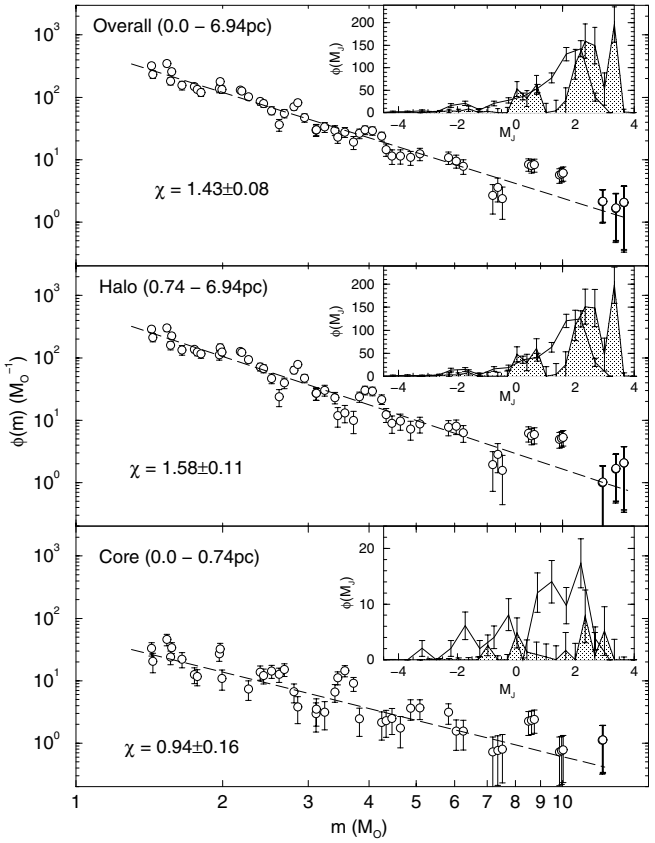

Fig. 8. Core, halo and overall mass functions of MS stars (empty circles) in NGC 4755. Each panel contains MFs combining J, H and K_s 2MASS photometry. MF fits $\left(\phi(m) \propto m^{-(1+\chi)}\right)$ are shown as dashed lines. Insets: MS (heavy-solid line) and PMS (shaded curve) field-star subtracted LFs. PMS stars are scarce in the core.

estimates (Cols. (10)–(12) in Table 1) are lower limits, since we do not have stars less massive than 1.4 $M_\odot$.

4.2. Deficiency of PMS stars in the core

During the early phases of PMS evolution, circumstellar DDEs are subject to several dissipation processes (Sect. 1). In principle these processes should depend on properties of the central star (mass, radius and luminosity), with no strong dependence on position in a star cluster. In this sense, the spatial distributions of MS and PMS stars should be similar. However, MS and PMS stars distribute differently through the body of NGC 4755, with the vast majority of PMS stars located in the halo (Figs. 7 and 8). The ratio number of PMS to MS stars is $\frac{N_{PMS}}{N_{MS}} \sim 0.25$ in the core, increasing to ∼1.2 in the halo. The apparent deficiency of the core PMS, compared to MS stars, may be linked to the denser environment, since the number-density of observed PMS + MS + Evolved stars in the core is $\eta_c \sim 26$ stars pc^{-3} while in the halo it drops to $\eta_h \sim 0.4$ stars pc^{-3} (Table 1). Such densities correspond to average distances between stars of ≈0.2 pc in the core and ≈0.9 pc in the halo. Processes that could provide additional dissipation mechanisms of PMS DDEs in the core include: *(i)* stellar density-enhanced radiation pressure, *(ii)* tidal disruption and *(iii)* primordial O stars.

4.2.1. Radiation pressure

Star clusters are not completely virialized systems. However, young clusters may reach some level of energy equipartition – particularly in the core – as suggested by King-like stellar RDPs, mass segregation and advanced dynamical states (e.g. Bonatto & Bica 2005). These conditions apply to NGC 4755 (Sect. 5). Below we assume a cluster virialized state only to derive an estimate of radiation pressure effects on DDEs.

In thermodynamic equilibrium radiation pressure relates to energy density as $P_r = \frac{1}{3}\varepsilon$. Assuming that uniformly distributed stars are the energy source in a spherical region with radius in the range (r_1, r_2), energy density can be estimated from $\varepsilon = \frac{1}{c}\int_{r_1}^{r_2} \eta \mathcal{F} 4\pi r^2 dr$, where η is the number-density of stars, $\mathcal{F} = \frac{L}{4\pi r^2}$ is the stellar flux at a distance r, and c is the speed of light. The average radiation pressure in the region is $\overline{P_r} \approx \frac{1}{3c}\eta\,\overline{L}(r_2 - r_1)$, where the average luminosity is calculated from the observed MFs (Fig. 8), $\overline{L} = \int L(m)\phi(m)dm / \int \phi(m)dm$, with the mass-luminosity relation $L(m)$ taken from the 14 Myr Padova isochrone. From Table 1 we derive $\overline{L_c} \approx 130\ L_\odot$ and $\overline{L_h} \approx 52\ L_\odot$, respectively for core and halo. We obtain $\overline{P_r}$(core) $\sim 1.2 \times 10^{-11}$ dyn cm^{-2}, and a core/halo ratio $\frac{\overline{P_r}(core)}{\overline{P_r}(halo)} \approx \left(\frac{\eta_c}{\eta_h}\right)\left(\frac{\overline{L_c}}{\overline{L_h}}\right)\left(\frac{R_c}{R_h}\right) \approx 20$, where $R_h = R_{lim} - R_{core}$ is the halo extension. This suggests that in the core the radiation field may be ∼20× harder to DDEs than the halo because of the uniform force exerted on dust particles (F_r) by the average radiation pressure. Because the radiation field in a cluster is nearly isotropic, the effective force acting on a dust grain is smaller than F_r. The ratio of the (upper limit) radiation force to the gravitational force acting on a spherical particle with radius r_d and density ρ_d located at a distance r from a star of mass M is $F_r/F_G \leq \frac{3P_r r^2}{4GM\rho_d r_d}$.

The mean composition of dust grains in young and old discs seems to resemble that of the solar system comets (as reviewed by Hillenbrand 2005), ∼70−80% amorphous magnesium-rich olivines, ∼1−10% crystalline forsterite, ∼10−15% carbons, ∼3−5% irons, and trace elements such as silicas. Densities of these elements are in the range $\rho_d \approx 2$−5 g cm^{-3}. Water ice with

$\rho_d \approx 1$ g cm^{-3} is another common element found in dust grains. In a favourable scenario for DDE disruption, a dust particle with $\rho_d = 1$ g cm^{-3} and $r_d = 1$ μm located at $r = 500$ AU (typical circumstellar disc radius – Hillenbrand 2005) from a $M = 1$ $M_\odot$ star will be subject to $F_r/F_G \leq 0.06$. For smaller disc radii and/or higher grain densities the ratio is even lower. Thus, the average radiation pressure in the core of NGC 4755 has only a marginal effect on circumstellar dust particles.

4.2.2. Tidal disruption

Tidal disruption is effective when the time between binary encounters is significantly shorter than the cluster age. For a dust particle located at a distance r from the center of a star, the tidal radius due to a second star is $r_t = 1.25$r. The effective volume ($\sim\eta_c^{-1}$) occupied by a star in the core is 0.04 pc^3. Taking r as the typical disc radius, a star with a tidal cross-section πr_t^2 traveling at $\approx$3 km s^{-1} will cover the effective volume in $\sim$100 Myr, about 8 times the cluster age. Thus, binary encounters in the core are not important as DDE disruption mechanism. However, a star located at the core radius feels the combined tidal pull of all core stars. This increases the tidal radius to $\approx 7\,r$ and the time between tidal encounters drops to $\sim$3 Myr. A more realistic estimate must be an intermediate value, suggesting that tidal disruption may have played a role in disrupting PMS DDEs in the core.

4.2.3. O stars

The few SGs of NGC 4755 (Sect. 2) evolved from massive stars. We cannot exclude the presence of other past massive stars that evolved into compact residuals. An intense radiation field of O stars, particularly in the UV, certainly eroded some DDEs in a short period ($\sim$4 Myr).

Perhaps the small amount of differential reddening in NGC 4755 (Sagar & Cannon 1995) is a relic of dissipated circumstellar envelopes by means of the processes discussed above.

5. Dynamical state of NGC 4755

Within uncertainties, the overall MF slope ($\chi = 1.43 \pm 0.08$) in the mass range $1.4 \leq m(M_\odot) \leq 13.5$ agrees with that of a Salpeter's ($\chi = 1.35$) IMF, and MF slopes present significant spatial variations, being flatter in the core and rather steep in the halo (Table 1 and Fig. 8). In older clusters this fact reflects dynamical mass segregation, in the sense that low-mass stars originally in the core are transferred to the cluster's outskirts, while massive stars sink in the core. This process produces a flat core MF and a steep one in the halo (e.g. Bonatto & Bica 2005).

Mass segregation in a star cluster scales with the relaxation time $t_{relax} = \frac{N}{8 \ln N} t_{cross}$, where $t_{cross} = R/\sigma_v$ is the crossing time, N is the (total) number of stars and σ_v is the velocity dispersion (Binney & Tremaine 1987). Relaxation time is the characteristic time-scale for a cluster to reach some level of energy equipartition. For a typical $\sigma_v \approx 3$ km s^{-1} (Binney & Merrifield 1998) we obtain $t_{relax} \approx 24 \pm 5$ Myr for the overall cluster and $t_{relax} \approx 0.4 \pm 0.1$ Myr for the core. The $\approx$14 Myr age of NGC 4755 (Sect. 3) corresponds to $\sim 40 \times t_{relax}$(core). Thus, some degree of MF slope flattening in the core is expected. However, the ratio cluster age to t_{relax} drops to $\sim$0.6 for the overall cluster, consistent with the Salpeter slope and absence of important large-scale mass segregation.

Bonatto & Bica (2005) derived a set of parameters related to the structure and dynamical evolution of open clusters in different dynamical states. They analysed nearby open clusters with ages in the range 70−7000 Myr and masses in 400−5300 $M_\odot$, following the methodology now employed. The evolutionary parameter τ = age/t_{relax} was found to be a good indicator of dynamical state. In particular, significant flattening in core and overall MFs due to dynamical effects such as mass segregation is expected to occur for $\tau_{core} \geq 100$ and $\tau_{overall} \geq 7$, respectively.

Figure 9 focuses on structural parameters, having in mind that mass and density values of NGC 4755 are lower limits (Sect. 4.1). The limiting radius is consistent with the low-limit correlation of R_{lim} with age (panel d). Although with a larger scatter, the same is observed in the correlation of R_{core} with age (panel e). The lower-limit of the core density of NGC 4755 follows the trend presented by massive clusters for young ages (panel a). A similar trend is seen for the overall density (panel b). In Galactocentric distance the limiting radius of NGC 4755 helps define a correlation (panel g) in the sense that clusters at larger d_{GC} tend to be larger (Lyngå 1982; Tadross et al. 2002). The large scatter in panel (h) precludes any conclusion with respect to a dependence of core radius with d_{GC}. NGC 4755 fits in the tight correlations of core and overall mass (panel i), and core and limiting radii (panel f). Bonatto & Bica (2005) found that massive and less-massive clusters follow different, parallel paths in the plane of core radius × overall mass. NGC 4755 follows the massive cluster relation (panel c). Further details on parameter correlations are given in Bonatto & Bica (2005).

Dynamical-evolution parameters of NGC 4755 are compared with those of other open clusters in different dynamical states in Fig. 10. NGC 4755 fits in the tight correlations of core and overall MF slopes (panel d), and core and overall evolutionary parameters (panel c). The young age and rather small Galactocentric distance of NGC 4755, together with those of NGC 6611, suggest a correlation of d_{GC} with age (panel g) that would agree with Lyngå (1982). The Salpeter-like overall MF slope of NGC 4755 is consistent with the relations for $\chi_{overall} \times M_{overall}$ and $\chi_{overall} \times$ age (panels a and i, respectively). The scatter in panel (h) does not allow inferences on the relation of χ_{core} with mass. With respect to the evolutionary parameters of NGC 4755, $\chi_{overall}$ follows the relation suggested by massive clusters with small values of τ (panel b). The core MF slope of NGC 4755 is flatter (1σ level) than the expected one for its value of τ (panel e). Core MF flattening with cluster age is illustrated in panel (f), where a higher flattening degree in the MFs of old less-massive clusters with respect to old massive ones occurs that probably reflects a looser stellar distribution. As they age, less-massive clusters tend to lose larger fractions of low-mass stars through internal processes (e.g. mass segregation and evaporation), and external ones (e.g. tidal stripping, disc shocking and encounters with molecular clouds – Bonatto & Bica 2005, and references therein). The locus occupied by the core MF of NGC 4755 is consistent with the cluster mass and age.

We conclude that both structurally and dynamically, the overall parameters of NGC 4755 are consistent with those expected of an open cluster more massive than 1000 $M_\odot$ and $\approx$14 Myr old. The same applies to core-structural parameters. The rather flat MF in the core, on the other hand, cannot result from dynamical mass segregation only, since $\tau_{core} \sim 40$ is rather small. This is similar to what is observed in the core of the very young open cluster NGC 6611 ($\chi_{core} \approx 0.6$ and $\tau_{core} \approx 2$). Primordial conditions associated with fragmentation of the parent molecular cloud must have played a role in defining the current core dynamical state. Additional support for this scenario is

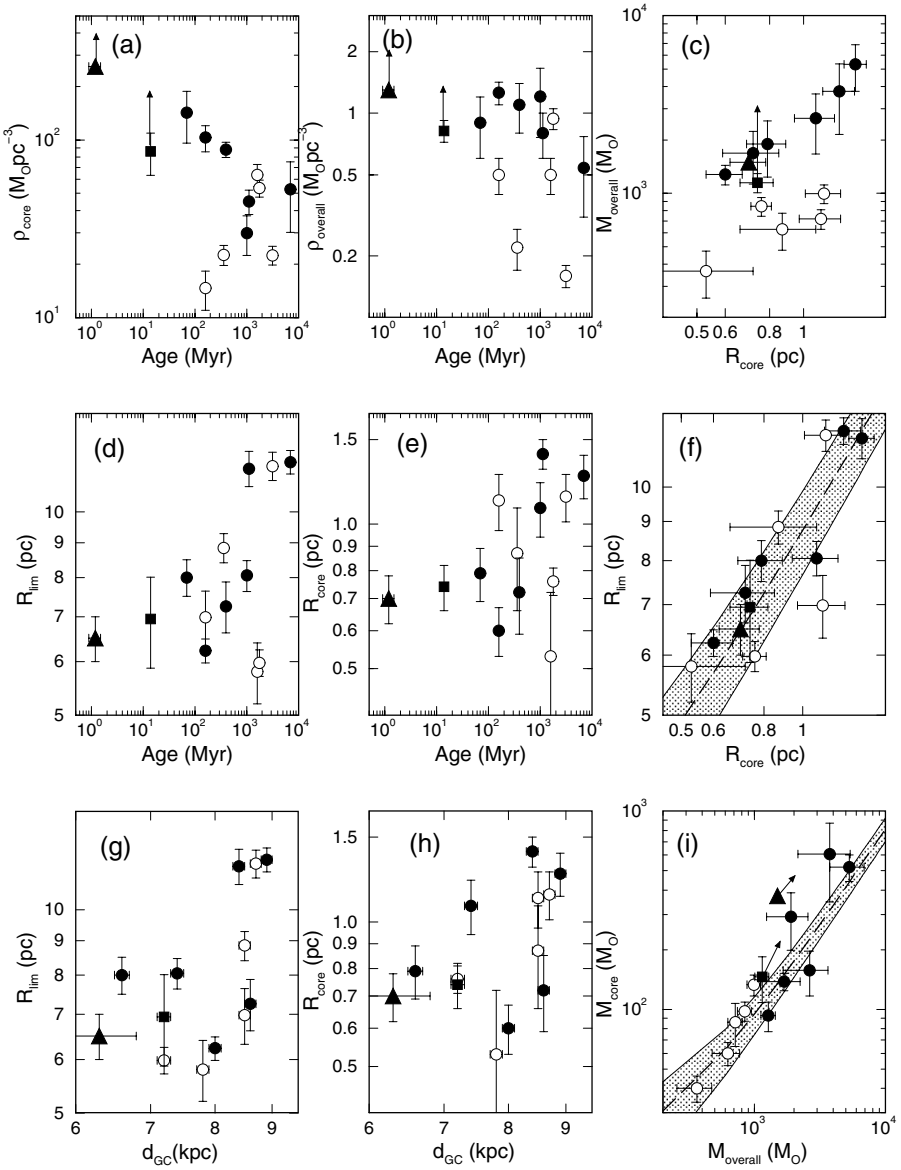

Fig. 9. Relations involving structural parameters of open clusters. Filled circles: clusters more massive than 1000 $M_{\odot}$. Open circles, $m < 1000\ M_{\odot}$. Filled triangle: NGC 6611. Filled square: NGC 4755. Dashed lines: least-squares fits to nearby clusters. Shaded areas: 1σ borders of least-squares fits. Arrows indicate lower-limit estimates of mass, density and evolutionary parameter for NGC 4755 and NGC 6611.

the near absence of binaries in the core compared to the halo of NGC 4755 (Sect. 3.5).

6. Concluding remarks

In this paper we analyzed the structure, membership and distribution of MS and PMS stars in the post-embedded young open cluster NGC 4755 by means of J, H and K_s 2MASS photometry and UCAC2 proper motions. Field-star decontamination was applied to the photometry to uncover the intrinsic CMD morphology. King's model fit to the MS radial density profile produced a core radius $R_{\rm core} = 0.74 \pm 0.08$ pc with a limiting radius $R_{\rm lim} \approx 6.9 \pm 1.1$ pc. Similar parameters were derived using PMS stars.

Field-star decontaminated CMDs present a well-defined MS with stars more massive than $\approx$1.4 $M_{\odot}$, ~285 candidate-PMS stars, 1 red SG and a few blue SG stars. A small fraction of MS and PMS stars present evidence of K_s-excess emission in this 14 Myr cluster. Cluster membership of candidate-PMS stars was confirmed by *(i)* their locus on the field-star decontaminated CMD, *(ii)* distribution on the 2-CD, *(iii)* cluster-like radial distribution of stars, and *(iv)* cluster-like proper-motion properties. Membership of K_s-excess MS and PMS stars was indicated by arguments *(i)* and *(iv)*. K_s-excess stars are absent in the core. From proper motions we found a significant number of binaries in the halo, but they are scarce in the core.

The halo MF of NGC 4755 is similar to a Salpeter IMF with a slope $\chi = 1.58 \pm 0.11$, while in the core it is flatter, $\chi = 0.94 \pm 0.16$. This change in MF slope implies that dynamical mass segregation has affected stellar distribution in the core, since the core-relaxation time $t_{\rm relax}$(core) ~ 0.35 Myr corresponds to only ~2.5% of the cluster age. For the overall cluster $t_{\rm relax}$(overall) ~ 24 Myr or ~1.7 × cluster age, which means that mass segregation did not have time to redistribute stars on a large scale throughout the halo of such a young cluster. The MF flattening in the core of NGC 4755 seems to be related to initial conditions, probably associated with the fragmentation of

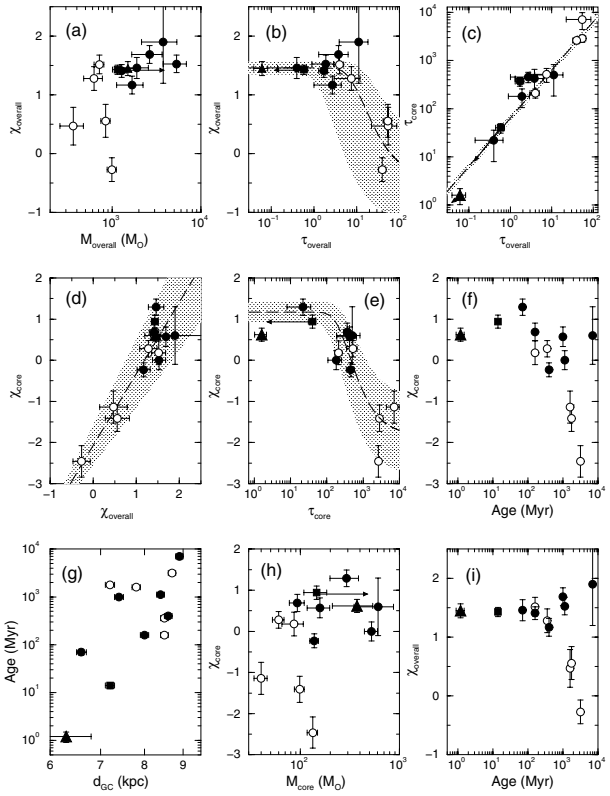

Fig. 10. Relations involving evolutionary parameters of open clusters. Symbols as in Fig. 9.

the parent molecular cloud, with more massive proto-stars preferentially located in the central parts of the cloud.

The age of NGC 4755 was constrained to 14 ± 2 Myr, consistent with low fractions of K_s-excess MS and PMS stars ($f_{K_s} \approx 5\%$). The observed mass locked up in MS, PMS and evolved stars is $(1.15 \pm 0.14) \times 10^3\ M_\odot$. Compared to MS stars there is a deficiency of PMS stars in the core of NGC 4755. The ratio of PMS to MS stars in the core is $\sim 1/5$ of that in the halo. Part of this can be accounted for by tidal disruption of DDEs in the stellar density-enhanced core, and/or the presence of O stars in the early phase of the cluster.

Comparing with theoretical tracks we detected member-PMS stars with ages in the range $\sim$1−14 Myr. This in turn implies that the star-formation time-scale in NGC 4755 is at least 10 Myr. If the main sources of K_s-excess emission are optically thick circumstellar dust discs, detection of K_s-excess in member MS stars indicates that the lifetime of some discs may be as large as the age of NGC 4755.

Acknowledgements. We thank the referee for helpful suggestions. This publication makes use of data products from the Two Micron All Sky Survey, which is a joint project of the University of Massachusetts and the Infrared Processing and Analysis Center/California Institute of Technology, funded by the National Aeronautics and Space Administration and the National Science Foundation. We also employed the WEBDA open cluster database and proper motion data from UCAC2 (The Second US Naval Observatory CCD Astrograph Catalog). C.B., E.B. and B.B. acknowledge support from the Brazilian Institutions CNPq and FAPESP. S.O. acknowledges the Italian Ministero dell'Università e della Ricerca Scientifica e Tecnologica (MURST), under the program on "Fasi Iniziali di Evoluzione dell'Alone e del Bulge Galattico" (Italy).

References

D'Alessio, P., Calvet, N., Hartmann, L., Lizano, S., & Cant, J. 1999, ApJ, 527, 893
Andrews, S. M., & Williams, J. P. 2005, ApJ, 631, 1134
Armitage, P. J., Clarke, C. J., & Palla, F. 2003, MNRAS, 342, 1139
Bica, E., & Bonatto, C. J. 2005a, A&A, 431, 943
Bica, E., & Bonatto, C. J. 2005b, A&A, 443, 465
Binney, J., & Tremaine, S. 1987, in Galactic Dynamics (Princeton, NJ: Princeton University Press), Princeton series in astrophysics
Binney, J., & Merrifield, M. 1998, in Galactic Astronomy (Princeton, NJ: Princeton University Press), Princeton series in astrophysics
Bonatto, C., & Bica, E. 2003, A&A, 405, 525
Bonatto, C. J., & Bica, E. 2005, A&A, 437, 483
Bonatto, C. J., Bica, E., & Pavani, D. B. 2004a, A&A, 427, 485
Bonatto, C., Bica, E., & Girardi, L. 2004b, A&A, 415, 571
Bonatto, C. J., Bica, E., & Santos, Jr., J. F. C. 2005, A&A, 433, 917
Bonatto, C. J., Santos, Jr., J. F. C., & Bica, E. 2006, A&A, 445, 567
Brandner, W., Zinnecker, H., Alcal, J. M., et al. 2000, AJ, 120, 950
Chen, C. H., Jura, M., Gordon, K. D., & Blaylock, M. 2005, ApJ, 623, 493
Dachs, J., & Kaiser, D. 1984, A&AS, 58, 411
Dutra, C. M., Santiago, B. X., & Bica, E. 2002, A&A, 381, 219
Girardi, L., Bertelli, G., Bressan, A., et al. 2002, A&A, 391, 195
Hillenbrand, L. A. 2005, in A Decade of Discovery: Planets Around Other Stars, STScI Symp. Ser. 19, ed. M. Livio, in press [arXiv:astro-ph/0511083]
Kenyon, S. J., & Hartmann, L. 1995, ApJS, 101, 117
King, I. 1966a, AJ, 71, 64
King, I. 1966b, AJ, 71, 276
Kroupa, P. 2002, Science, 295, 82
Kroupa, P. 2004, New Astron. Rev., 48, 47
Lada, C. J., & Adams, F. C. 1992, ApJ, 393, 278
Low, F. J., Smith, P. S., Werner, M., et al. 2005, ApJ, 631, 1170
Lyngå, G. 1982, A&A, 109, 213
Lyngå, G. 1987, in Catalog of Open Cluster Data, Computer Based Catalogue available through the CDS, Strasbourg, France and NASA DATA Center, Greenbelt, Maryland, USA, 5th edition, 4, 121
Mermilliod, J. C. 1996, in The Origins, Evolution, and Destinies of Binary Stars in Clusters, ed. E. F. Milone, & J.-C. Mermilliod, ASP Conf. Ser., 90, 475
Nilakshi, S. R., Pandey, A. K., & Mohan, V. 2002, A&A, 383, 153
Ortolani, S., Bica, E., Barbuy, B., & Momany, Y. 2005, in Protostars and Planets V, ed. B. Reipurth, Kona, Hawaii
Piskunov, A. E., Belikov, A. N., Kharchenko, N. V., Sagar, R., & Subramaniam, A. 2004, MNRAS, 349, 1449
Reid, M. J. 1993, ARA&A, 31, 345
Sagar, R., & Cannon, R. D. 1995, A&AS, 111, 75
Sanner, J., Bruzendorf, J., Will, J.-M., & Geffert, M. 2001, A&A, 369, 511
Schmidt-Kaler, T. 1982, in Landolt-Börnstein, New Ser., Group VI (Berlin: Springer-Verlag), Vol. 2b, 1
Salpeter, E. 1955, ApJ, 121, 161
Siess, L., Dufour, E., & Forestini, M. 2000, A&A, 358, 593
Skrutskie, M., Schneider, S. E., Stiening, R., et al. 1997, in The Impact of Large Scale Near-IR Sky Surveys, ed. Garzon et al. (Netherlands: Kluwer), 210, 187
Tadross, A. L., Werner, P., Osman, A., & Marie, M. 2002, NewAst, 7, 553
Trager, S. C., King, I. R., & Djorgovski, S. 1995, AJ, 109, 218
White, R. J., & Hillenbrand, L. A. 2005, ApJL, 621, 65
Zacharias, N., Urban, S. E., Zacharias, M. I., et al. 2004, AJ, 127, 3043